32ND INTERNATIONAL COSMIC RAY CONFERENCE, BEIJING 2011

Estimation of effective aperture for extreme energy cosmic ray observation by JEM-EUSO Telescope

K. SHINOZAKI[1,2], M.E. BERTAINA [3], S. BIKTEMEROVA[4], P. BOBIK[5], F. FENU[6,1], A. GUZMAN[7], K. HIGASHIDE[8,1], G. MEDINA TANCO[7], T. MERNIK[6], J.A. MORALES DE LOS RIOS PAPPA[2], D. NAUMOV[4], M.D. RODRIGUEZ - FRIAS[2], G. SAÉZ CÁNO[2] AND A. SANTANGELO[6] ON BEHALF OF JEM-EUSO COLLABORATION

[1]*Computational Astrophysics Laboratory, RIKEN Advanced Science Institute, 2-1 Hirosawa, Wako 351-0198, Japan*
[2]*Space and Astroparticle Group (SPAS), University of Alcala, E-28807 Alcalá de Hénares, Spain*
[3]*Department of General Physics, University of Torino, Via P. Giuria 1, I-10125 Turin, Italy*
[4]*Joint Institute for Nuclear Research, Joliot-Curie 6, 141980 Dubna, Moscow Region, Russia*
[5]*Institute of Experimental Physics, Slovak Academy of Science, 040 01 Kosice, Slovakia*
[6]*Institut für Astronomie und Astrophysik, Eberhard-Karls Universität Tübingen, Sand 1, D-72076 Tübingen, Germany*
[7]*Institudo de Ciencias Nucleasres, Universitat Natcional Autonoma Mexico, Mexico City 04510, Mexico*
[8]*Department of Physics, Saitama University, Saitama 338-8570, Japan*

kenjikry@riken.jp

DOI: 10.7529/ICRC2011/V02/0979

Abstract: JEM-EUSO (Extreme Universe Space Observatory on Japanese Experimental Module) is a space-based new type observatory to explore the extreme-energy-region Universe in particle channel. In the present work, we estimated the effective aperture of the current baseline configuration of the JEM-EUSO telescope in observing extreme energy cosmic rays. We tested the effect of the qualty cut among observed extensive air showers for cross-calibration with other experiments. We also demonstrated several advanges for the space-based JEM-EUSO observation.

Corresponding authors:

Keywords: Extreme energy cosmic rays, JEM-EUSO, extensive air showers

1 Introduction

The origin and existence of extremely energetic cosmic rays (EECRs; referred to as ones with energies E_0 several $\sim 10^{19}$ eV and higher) remains an open puzzle in the contemporary astroparticle physics. Possible indications of sources or excess of EECRs in Celestial Sphere have been claimed by ground-based experiments [1, 2, 3], despite that capable sources are most powerful objects within limited distances by the Greisen-Zatseptin-Kuzmin effect [4, 5]. To investigate this puzzle, studies of energy spectrum and arrival directions of EECRs against their extremely low fluxes of 1 or fewer in km^2 per century, are essential. The size of observation area is therefore critical factor.

JEM-EUSO (Extreme Universe Space Observatory onboard Japanese Experiment Module) is the observatory for EECRs [6, 7]. The JEM-EUSO telescope will be accommodated on JEM/Exposed Facility of the International Space Station (ISS). The scientific objectives include astronomy and astrophysics through EECR channel and other exploratory objectives [8] such as detection of extreme energy gamma rays and neutrinos.

By means of air fluorescence technique, the observation of EECRs depends upon extensive air showers (EASs) phenomenon initiated by primary EECRs. This technique has been developed by several ground-based fluorescence telescopes, however, never been practiced in space. From the orbit, EAS event is observed as a luminous spot moving at the speed of light. For the event with an energy $E_0 = 10^{20}$ eV, for example, the EAS development results in emission of an order of 10^{16} fluorescence photons depending on the zenith angle θ of EAS. The telescope receives an order of thousands of photons per square meter aperture.

By monitoring night Earth with a wide field-of-view (FOV) telescope, a series of advantages and scientific merits are expected. When the JEM-EUSO telescope points to the nadir (nadir mode), unique geometry between EAS and telescope provides less uncertainty in EAS reconstruction due to well-constrained EAS-to-telescope distance. Observations over the orbit will cover the entire Celestial Sphere that allows searching any direction for EECR sources and

for global arrival direction distribution. For scientific objectives, the most essential merit is the observation area far larger than ground-based telescope. We also plan to tilt the telescope off the nadir toward the horizon (tilt mode) that enhances the projected FOV on the Earth's surface to allow more effective observation at higher energies.

In the present work, we focus on the aperture of the JEM-EUSO trigger system for EECR observation. We will discuss relevant issues to estimate the exposure of the data.

2 Apparatus and observation conditions

Apparatus The main part of the JEM-EUSO telescope consists of an $\sim$ 4-m^2-aperture optics with three Fresnel lenses [9] with aspherical curved focal surface (FS) covered by about 137 photodetector modules (PDMs) [10]. Each PDM is composed with 36 multi-anode photomultiplier tubes (MAPMTs) with ultra-bialkali photocathode with 64 channels [11]. PDMs are aligned on FS to maximize the observation area. In the baseline design, about 5000 MAPMTs are deployed and thus the total number of pixels is $\sim 3 \times 10^5$. symmetrically cut with a 40° segment. The spatial resolution for each pixel corresponds to $\sim 0.07^\circ$ or ~ 0.5 km on the Earth's surface for an orbit altitude $H_{\rm ISS} \sim 400$ km. For each pixel, data is acquired with every 2.5 μs (gate time unit) when the two consecutive levels of trigger schemes are activated[12]. These trigger schemes are referred to persistent track trigger (PTT) and line track trigger (LTT). Each scheme searches individual PDM for localized or aligned excesses of signals. Threshold levels for PTT and LTT are dynamically set to fit the rates within hardware requirement and telemetry budget.

Orbit and observation area The orbit of the ISS has an inclination $i = 51.6^\circ$ with $H_{\rm ISS}$ ranging in 278–460 km by the operational limit. The sub-satellite speed and period are $\sim$ 7 km/s and $\sim$ 90 minutes, respectively. Apart from effects by orbital decay and operational boost-up, the ISS motion is approximated as a circular motion with an eccentricity of practically 1. Among these elements, $H_{\rm ISS}$ is widely variable throughout its operation and so far has range between ~ 350 and ~ 400 km.

The 'observation area' of JEM-EUSO which depends upon tilting angle ξ off the nadir and $H_{\rm ISS}$ is estimated by ray trace simulations [9, 13] for isotropic light source viewed by the FS detectors. In the following we defined it as the projected area on the Earth's surface from which the main ray of photons are detected within outer most boundaries of the FS detector.

Figure 1 shows the observation area as a function of tilting angle for different $H_{\rm ISS} = 350, 400$ and 430 km.

For the baseline layout of 137 PDMs, the observation area $A_{\rm obs}^{\rm (nadir)}$ for nadir mode is a function of $H_{\rm ISS}$ expressed by:

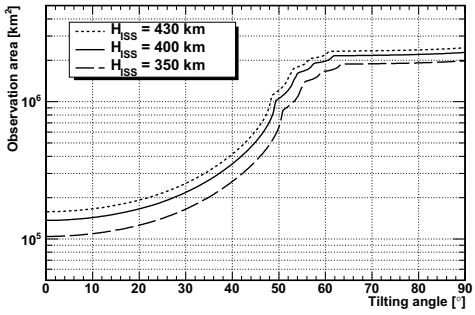

Figure 1: Observation area as a function of tilting angle for different altitudes of 400 km (solid line), 350 km (dashed line) and 430 km (dotted line).

$$A_{\rm obs}^{\rm (nadir)}[{\rm km}^2] \approx 1.4 \times 10^5 \cdot \left(\frac{H_{\rm ISS}}{400[{\rm km}]} \right)^2 \qquad (1)$$

With tilting angles ξ up to $\sim 40^\circ$, the observation area $A_{\rm obs}$ is approximated as follows:

$$A_{\rm obs}(\xi) \approx A_{\rm obs}^{\rm (nadir)} (\cos \xi)^{-b} \qquad (2)$$

where b ranges 3.2–3.4 for the altitude of interest. In this region $A_{\rm obs}$ increases with ξ. Around $xi \sim 40-50$ degrees depending upon $H_{\rm ISS}$, a part of FOV views the sky over the local horizon and $A_{\rm obs}$ saturates above $\xi \sim 60^\circ$.

Background and cloud impact The level of background (BG) noise is a key parameter to define the observation and schemes that yields the observation duty cycle η_0 as well. The first order constraint for η_0 is astronomically determined by the ISS transit over terminator. For $H_{\rm ISS} \sim 400$ km, the average fraction of nighttime is $\sim 33\%$ at the orbital altitude. By applying the upper limit of the BG flux in UV range of 300–400 nm less than 1500 photon m^{-2} sr^{-1}, η_0 corresponds to $\sim 20\%$ (see [15] for details). In this criterion, the average background flux is ~ 500 photons m^{-2} sr^{-1} ns^{-1} (referred to 'average BG level'). Note that the presence of the Moon with its phase close to New Moon is included in operational time as JEM-EUSO telescope is only affected by the illumination of Earth's surface.

The impact of clouds is estimated by the global secular statistics of the optical depth and cloud-top altitude [16] convolved with the trigger probability for each case. The trigger aperture for the time-average cloudy condition is $\sim 80\%$ above $\sim 5\times10^{20}$ eV in comparison with that for the cloud-free case. Applying quality cut for events with shower maximum above the optically thick clouds, the overall impact factor is estimated to be $\kappa_{\rm C} \sim 70\%$ above 3×10^{19} eV (see [17] for details).

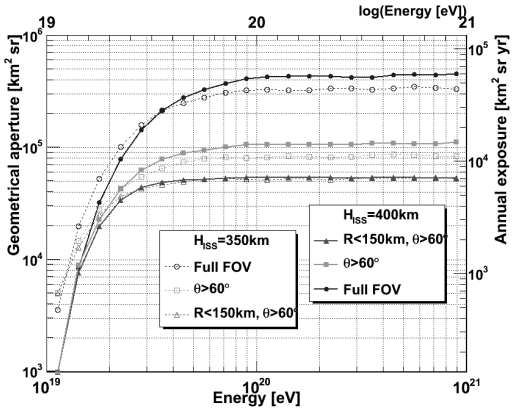

Figure 2: Geometrical aperture as a function of E_0. Open and closed circles indicate geometrical apertures for the ISS altitudes of 400 and 350 km, respectively. Squares and triangles show the cases of different geometrical cuts of $\theta > 60^\circ$ and $R < 150$ km, respectively. The vertical axis on the right represent annual exposure taking into account observation duty cycle and cloud impact.

3 Simulation and results

Simulation In the present work, we employed the ESAF (Euso Simulation and Analysis Framework) [18, 19] adapted into the present JEM-EUSO baseline configuration. The software is written in C++ using an object-oriented programming approach and runs on the ROOT package [20]. EAS generation is based on the GIL (Greisen-Ilina-Linsley) formulation [21] that reproduced the longitudinal development of hadronic showers simulated by CORSIKA [22] with QGSJET interaction model [23]. Fluorescence yield is a well recognized uncertainty for energy scale [24, 25]. In the present work, we assumed it by Nagano *et al.*[26]. To estimate trigger aperture, we simulated a large number of EAS uniformly injected into an area far larger than $A_{\rm obs}^{\rm (nadir)}$. $H_{\rm ISS}$ is set to be 350 and 400 km. Threshold levels for PTT and LTT trigger judgements need to fit within permissible fake trigger rates, while it is preferable to keep as low as possible. For optimizations of those parameters, we generated a large amount of noise simulations by STM code [13].

Geometrical aperture Unless otherwise noted, we define 'geometrical aperture' based on the probability satisfying second level LTT trigger condition by means of Monte Carlo simulations. The time-variant conditions such as cloud coverage or BG level are excluded in definition. In the present work, we assume the clear sky condition with average BG level. The exposure growth per given time may be evaluated by a product of η_0 and $\kappa_{\rm C}$ in the previous section. The estimation herein is a preliminary result for the current baseline detector configuration for the nadir mode.

For $N_{\rm trig}$ trigger events among simulated $N_{\rm inject}$ injected EECRs with an energy E_0, the corresponding geometrical aperture $A(E_0)$ is defined as follows:

$$A(E_0) = \frac{N_{\rm trig}}{N_{\rm inject}} \cdot S_0 \cdot \Omega_0 \qquad (3)$$

where S_0 and $\Omega_0 = \pi$ [sr] for $\theta = 0^\circ - 90^\circ$ are the area and the effective solid angle, respectively, in which uniform EAS flux is assumed. To evaluate full geometrical aperture, we applied $S_0 \gg A_{\rm obs}$ to take into account EAS crossing FOV with a core location out of the observation area.

By applying the geometrical selection for good quality events by core location distance R from the center of FOV and lower limit of zenith angle $\theta_{\rm cut}$, subset of geometrical aperture for a given energy is expressed as follows:

$$A_{\rm sub} \propto \int_0^{R_{\rm max}} \int_{\theta_{\rm cut}}^{90^\circ} \epsilon(\theta, \vec{r}) \cdot \sin\theta \cos\theta d\theta \cdot r dr \qquad (4)$$

where $\epsilon(\theta, \vec{r})$ is the probability of trigger at the location of $\vec{r}$ with respect to the correspoding position on Earth's surface to the center of FOV. The amount of light produced in EAS increases with zenith angle since the apparent EAS track becomes longer before being truncated at Earth's surface. In the inner part of FOV, higher efficiency in trigger is expected due to better focusing power of the optics along with shorter EAS-to-telescope distance.

Figure 2 shows the geometrical aperture as a function of E_0 for $H_{\rm ISS} = 400$ and 350 km. Effects of different geometrical cuts in θ and R are also demonstrated. The scale of annual exposure (growth in exposure by one-year operation) is also shown on the right by taking into account $\eta_0 = 0.2$ and $\kappa_{\rm C} = 0.7$ (see caption and legend for details).

At highest energies, the geometrical aperture for full FOV is almost constant above $\sim (6-7) \times 10^{19}$ eV. The saturated aperture is determined by $A_{\rm obs}$ for given $H_{\rm ISS}$ and therefore the higher altitudes result in the larger apertures. Comparing annual exposure to the Auger (7000 km^2 sr yr) [14], it is expected to be ~ 9 times for $H_{\rm ISS} = 400$ km.

Applying $\theta_{\rm cut} = 60^\circ$ cut to full FOV, while the effective solid angle reduces to $\pi/4$ [sr], almost constant aperture is achieved above $\sim (4-5) \times 10^{19}$ eV. In addition, more stringent $R_{\rm max} = 150$ km cut extends such range down to $\sim (2-3) \times 10^{19}$ eV. It is worthy to mention that for lower $H_{\rm ISS}$ shorter EAS-to-telescope distances increases $\epsilon(\theta, \vec{r})$ for the same energy. This results in the larger apertures and enable better comparison with other experiments in more extended energy range.

Uniformity of exposure Unlike stationary ground-based observatories, global ISS orbit and better sensitivities for large θ EAS allow to scan the entire Celestial Sphere. The exposure distribution is practically flat in right accession. Apart from possible local or seasonal deviation from the global average of cloud coverage and BG level, the relationship between expected overall exposure and declination

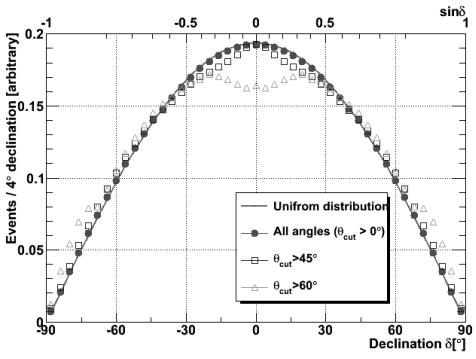

Figure 3: Declination δ distribution of triggered events for different $\theta_{\rm cut} = 0^\circ$ (circles), 45° (squares) and 60° (triangles) in comparison with uniform distribution (solid curve). The horizontal axis on the top shows $\sin\delta$ to indicate the solid angle coverage on the Celestial Sphere.

can be analytically expressed as a function of only $\theta_{\rm cut}$, knowing observable night time at a given latitude.

Figure 3 shows expected distribution of triggered events in declination for different $\theta_{\rm cut} = 0^\circ$, 45° and 60° cuts compared with uniform distribution.

For the case of $\theta_{\rm cut} = 60^\circ$ cut, minor excesses and deficit may arise in very limited parts near Celestial Poles and Equator, respectively. It is because sinuous variation in latitude of the orbit and JEM-EUSO stays longer in high latitudes. JEM-EUSO can achieve well constant exposures for full range of θ with which arrival direction analysis will be made. In the case of ground observatories, first of all they are constrained in observation of never-rising region below the local horizon and the correction factor for non-uniform observable region may even reach ~ 3.

4 Summary and discussion

In the present work, we simulated a large number of EAS to estimate the effective aperture for present baseline configuration and argued the relevant issues. $A_{\rm obs}^{\rm (nadir)}$ is proportional to the square of $H_{\rm ISS}$ which is highly dependent upon the ISS operation. In the mission, the science case has assumed $H_{\rm ISS}$ to be either ~ 400 km, or 430 km following the prediction at the time of EUSO mission [27]. In case of lower altitudes such as 350 km, $A_{\rm obs}$ is compensated by tilting $\sim 25^\circ$ to that of the nadir mode at 430 km altitude without dramatic change of EAS-to-telescope distance.

The geometrical aperture was estimated for clear sky condition. It is important to mention that applying geometrical cuts helps discriminate good quality events in the energy range $(2-3)\times 10^{19}$ eV at constant exposure with energy. Such subset of EAS data makes it possible to cross-check energy spectrum and performances with ground-based experiments at equivalent statistical power. Once it is carried, exposure at higher energies overwhelm by removing such cuts. Taking int account factors of η_0 and $\kappa_{\rm C}$, ~ 9 times annual exposure is expected in comparison with that of Auger. Particularly to increase the statistics at highest energies $\sim (3-5)\times 10^{20}$ eV, we plan to operate the telescope in tilt mode and also with higher BG level threshold.

The full coverage of EECR observation in Celestial Sphere is unique characteristics for the JEM-EUSO and moreover the overall exposure results in almost uniform at the first order. Such an advantage is more pronounced for arrival direction analysis, especially against spread EECR sources.

Some results shown herein are in progress. Further details on the general performance can be also referred in [28].

Acknowledgement

KS wishes to express his gratitude to University of Alcalá (UAH), Eberhard-Karls Universität Tübingen and University of Torino for their hospitality and excellent working conditions. Computation facilities of RICC (RIKEN Integrated Cluster of Clusters) System and of UAH-SPAS are acknowledged for efficiently performing simulations. The present work was supported in part by the Italian Ministry of Foreign Affairs, General Direction for the Cultural Promotion and Cooperation.

References

[1] M. Takeda *et al.*, Astrophys. J, 522, 255 (1999).
[2] J. Abassi *et al.*, Astropart. Phys., 30, 175 (2009).
[3] J. Abraham *et al.* (Auger Collaboration), Proc. 31st Int. Cosmic Ray Conf (Lodz), arXiv:0906.2347.
[4] K. Greisen, Phys. Rev. Lett. 17, 748 (1966).
[5] G.Zatsepin and V.A.Kuzmin, J. Experimental and Theor. Phy., Lett. 4, 78 (1966).
[6] Y. Takahashi *et al.*, New J. Phys. 11, 065009 (2009).
[7] T. Ebisuzaki *et al.*, in these proceedings, #0120.
[8] G. Medina-Tanco *et al.*, in these proceedings, #0956.
[9] A. Zuccaro Marchi *et al.*, in these proceedings, #0852.
[10] M. Casolino *et al.*, in these proceedings, #1219.
[11] Y. Kawasaki *et al.*, Nucl. Instr. and Meth., A564, 378 (2006).
[12] J. Bayer, in these proceedings, #0836.
[13] K. Higashide *et al.*, in these proceedings, #1240.
[14] Auger Collaboration, in these proceedings.
[15] P. Bobik *et al.*, in these proceedings, #0886.
[16] F. Garino *et al.*, in these proceedings, #0398.
[17] G. Saez Cano *et al.*, in these proceedings, #1034.
[18] C. Berat *et al.*, Astropart. Phys., 33, 221 (2010).
[19] F. Fenu *et al.*, in these proceedings #0592.
[20] R. Brun *et al.*, Nucl. Inst. Meth. A389, 81 (1997).
[21] N.P Ilina et at., Soviet J. Nud. Phys 55, 1540 (1992).
[22] D. Heck and J. Knapp 1998, Forschungszentrum Karlsruhe Report, FZKA 6019 (1998).
[23] S. Ostapchenko, Phys.Rev. D 74, 014026 (2006).

[24] Eg for review, F. Arqueros, J. Hörandel and B. Keilhauer, Nucl. Instr. Meth. A597, 1 (2009).
[25] N. Sakaki *et al.*, in these proceedings, #0520.
[26] M. Nagano *et al.*, Astropart. PHys., 22, 235 (2004).
[27] EUSO Collaboration, *EUSO Proposal: Report on the Phase A Study*, 2002.
[28] A. Santangelo *et al.*, in these proceedings, #0991.